# Reliable Power Exchange in Energy Storage Systems using Multiport Bidirectional SEPIC–Luo Converter with PI Control Strategy

**Parvathi R. V. L. N. S., Gowthami K., Tejeswararao P., Abhishek G., Subrahmanyam E. S. N.**

Godavari Institute of Engineering and Technology (A),

Rajahmundry, India.

***Abstract.*** The main objective of this study is to develop a high-efficiency bidirectional DC-DC converter capable of ensuring reliable power exchange within Energy Storage Systems (ESS) and improving the lifespan of series-connected batteries through precise management of charging and discharging processes. The proposed work aims to achieve stable voltage–current regulation and effective battery protection under varying load and supply conditions. To accomplish these objectives, a Multiport Bidirectional Single Ended Primary Inductor Converter (SEPIC)–Luo Converter (MB-SLC) is designed, which operate efficiently in both boost and buck modes. In addition, a cascaded Proportional–Integral (PI) control architecture is implemented for regulating the voltage, the current, and the State of Charge (SOC) with high precision. The proposed converter and control performance are validated through MATLAB/Simulink simulations conducted under diverse operating scenarios. The results demonstrate smooth voltage and current profiles, rapid transient response, accurate SOC tracking, reduced ripple levels, and high conversion efficiency of 96% in step-up mode and 95.7% in step-down mode. These outcomes confirm the ability of the proposed system to maintain reliable power exchange while minimizing stress on the battery. The significance of the obtained results lies in their contribution to enhancing battery protection, extending operational lifespan, and providing a robust solution for renewable energy–integrated ESS. By combining advanced converter topology with cascaded PI control, the study offers a practical and scalable approach to improving energy storage reliability, efficiency, and sustainability.

***Keywords:*** energy storage system, multiport bidirectional SEPIC–Luo converter, proportional–integral, state of charge. boost mode, buck mode.

**DOI: https://doi.org/10.52254/1857-0070.2026.1-69.02**
**UDC: 621.3**

### Schimb fiabil de energie în sistemele de stocare a energiei utilizând un convertor SEPIC-Luo bidirecțional multiport cu strategie de control PI

**Parvathi R. V. L. N. S., Gowthami K., Tejeșwararao P., Abhișek G., Subrahmanyam E. S. N.**
Institutul de Inginerie și Tehnologie Godavari (A), Rajahmundry, India

***Rezumat.*** Obiectivul principal al acestui studiu este de a dezvolta un convertor CC-CC bidirecțional de înaltă eficiență, capabil să asigure un schimb fiabil de energie în cadrul Sistemelor de Stocare a Energiei (ESS) și să îmbunătățească durata de viață a bateriilor conectate în serie prin gestionarea precisă a proceselor de încărcare și descărcare. Lucrarea propusă își propune să realizeze o reglare stabilă a tensiunii-curentului și o protecție eficientă a bateriei în condiții variabile de sarcină și alimentare. Pentru a atinge aceste obiective, este proiectat un convertor SEPIC (Multiport Bidirectional Single Ended Primary Inductor Converter)-Luo Converter (MB-SLC), care funcționează eficient atât în modul boost, cât și în modul buck. În plus, este implementată o arhitectură de control proporțional-integral (PI) în cascadă pentru reglarea tensiunii, curentului și a stării de încărcare (SOC) cu precizie ridicată. Performanța convertorului și a controlului propus este validată prin simulări MATLAB/Simulink efectuate în diverse scenarii de funcționare. Rezultatele demonstrează profiluri line de tensiune și curent, răspuns tranzitoriu rapid, urmărire precisă a SOC, niveluri reduse de ondulație și o eficiență ridicată a conversiei de 96% în modul step-up și 95,7% în modul step-down. Aceste rezultate confirmă capacitatea sistemului propus de a menține un schimb de energie fiabil, minimizând în același timp solicitarea asupra bateriei. Semnificația rezultatelor obținute constă în contribuția lor la îmbunătățirea protecției bateriei, extinderea duratei de viață operaționale și furnizarea unei soluții robuste pentru sistemele de stocare a energiei (ESS) integrate în energie regenerabilă. Prin combinarea topologiei avansate a convertorului cu controlul PI în cascadă, studiul oferă o abordare practică și scalabilă pentru îmbunătățirea fiabilității, eficienței și sustenabilității stocării energiei.

***Keywords:*** sistem de stocare a energiei, convertor SEPIC–Luo bidirecțional multiport, proporțional–integral, stare de încărcare, mod boost, mod buck.

**Надежный обмен электроэнергией в системах накопления энергии с использованием многопортового двунаправленного преобразователя SEPIC–Luo со стратегией ПИ-регулирования**

**Парвати Р. В. Л. Н. С., Гаутами К., Теджешвাрарао П., Абхишек Г., Субрахманьям Э. С. Н.**
Инженерно-технологический институт Годавари (А), Раджамандри, Индия.

***Аннотация.*** Основная цель данного исследования — разработка высокоэффективного двунаправленного DC/DC-преобразователя, способного обеспечить надежный обмен энергией в системах накопления энергии (ESS) и увеличить срок службы последовательно соединенных аккумуляторов за счет точного управления процессами зарядки и разрядки. Предлагаемая работа направлена на достижение стабильного регулирования напряжения и тока и эффективной защиты аккумулятора при изменяющихся условиях нагрузки и питания. Для достижения этих целей разработан многопортовый двунаправленный однотактный первичный индуктивный преобразователь (SEPIC) — Luo-преобразователь (MB-SLC), который эффективно работает как в повышающем, так и в понижающем режимах. Кроме того, реализована каскадная архитектура пропорционально-интегрального (ПИ) управления для регулирования напряжения, тока и состояния заряда (SOC) с высокой точностью. Предлагаемый преобразователь и характеристики управления проверены с помощью моделирования MATLAB/Simulink, проведенного в различных рабочих сценариях. Результаты демонстрируют плавные профили напряжения и тока, быструю переходную характеристику, точное отслеживание уровня заряда батареи, сниженный уровень пульсаций и высокую эффективность преобразования: 96% в повышающем режиме и 95,7% в понижающем. Эти результаты подтверждают способность предлагаемой системы обеспечивать надежный обмен энергией, минимизируя нагрузку на аккумулятор. Значимость полученных результатов заключается в их вкладе в улучшение защиты аккумулятора, продление срока службы и обеспечение надежного решения для интегрированной системы накопления энергии с использованием возобновляемых источников энергии. Сочетание усовершенствованной топологии преобразователя с каскадным ПИ-регулированием позволяет предложить практичный и масштабируемый подход к повышению надежности, эффективности и устойчивости систем накопления энергии.

***Ключевые слова:*** *с*истема накопления энергии, многопортовый двунаправленный преобразователь SEPIC–Luo, пропорционально-интегральный, состояние заряда, режим повышения, режим понижения.

## I. INTRODUCTION

The DC power supplies are unstable, which translates to poor efficiency under unpredictable operational conditions, and excessive energy production under low demand periods [1]. These fluctuations result in periods of insufficient SOC and overload. Therefore, in order to account for these fluctuations and ensure a balanced energy demand and generation, ESS are considered the most realistic and efficient solution, that presents sufficient opportunity to optimize energy management and subsequently mitigate energy spillage. ESS are predominantly designed to capture energy from many sources, which is convert and store the energy in a format for different applications [2-3]. Also, it’s part of today's power systems around the world, and allow for reliable, flexible, and efficient energy management for a broad-spectrum application. In terms of common technologies of ESS, the electrochemical storage that includes batteries and super capacitors [4]. Super capacitors are used for high power density, fast charge/discharge abilities, prolonged life cycles, while its limitations by lower energy capacity, higher cost. Thus, batteries, particularly in lithium-ion batteries are typically adopted based on their energy density, lower form factor, and more established manufacturing eco system [5-6].

The Battery Energy Storage Systems (BESS) have an important position to store energy configured in actual flexible ways to meet different application requirements without geographic constraints. It has a fast response time handle both active and reactive power at the input and output simultaneously [7].

In comparison, BESS has a relatively high energy efficiency compared to other energy systems. These advantages make BESS an irreplaceable solution in centralized and distributed renewable energy integration [8].

The growing EV industry in recent years has driven battery manufacturing and application technology to a great range. Additionally, battery storage has become the most widely used and rapidly expanding form of energy storage innovation due to concerns about cost and battery life [9].

However, battery systems face operational difficulties, including cell imbalance due to variation in inherent capacity, internal resistance, self-discharge, and temperature gradients. Without proper means to control the balance, some cells either be over-charged or overdischarged, thus resulting in less capacity, greater aging and possibly safety risks [10]. The situation is complicated even further if a DC supply is connected directly to the battery for charging without any control in place [11]. Thus, it is interrupted creating further potential complications with over charging, over current and voltage imbalance, overheating and alternating reverse current when the supply. This condition of mechanisms surely degrade performance, decrease operating lifetime, and compromise safety. To mitigate these issues, BDCs are connected to the battery. A BDC allows for both a onward and backward power flow in a single converter and allows voltage step-up and step-down as needed. This feature of BDCs reduces the size of the entire system and improves efficiency [12-13]. Benefits of a BDC make it applicable in all applications that require current flow in both directions. Primary functions of BDCs include to supply the load with transient and overload power from the battery in forward power, and to re-charge a battery in reverse mode [14].

*A. Literature survey*

**K. Suresh *et al* (2025)** [15] have developed a high-efficiency and non-inverting step-down/step-up BDC converter system with mode change automatically for series-connected battery systems. The design supports increases energy conversion efficiency, load capability and protection for the transistor gate with a capacitive coupling level shift circuit. The performance of the design is affected by more complicated mode control and the need for precise frequency compensation to avoid instability. **Hsuan Liao *et al* (2022)** [16] have created a BDC converter with a rapid energy bidirectional transition technology to allow smooth and safe changes in power direction in DC distribution and ESS. The converter utilizes an LC resonance-based path to accomplish fast energy transfer without surges, while achieving a high-power conversion ratio with a basic circuit construction. However, the isolated driver circuit increase the complexity between the battery side and DC bus side, which increases complexity in the system. **Sara Mousavinezhad Fardahar *et al* (2020)** [17] have designed a high step-down/step-up interleaved BDC to attain lower voltage stress on semiconductor switches. The converter topology with coupled inductors and blocking capacitors enables high voltage gain, simple control, and uniform voltage gain characteristics throughout the duty cycle range. However, its structure and a parallel module arrangement which is increase the design complexity and component count. **Muhammad Zeeshan Malik *et al* (2023)** [18] have proposed a coupled-inductor-based high step-up/high step-down BDC converter design for EV battery applications. Their design achieved fewer components, and less voltage stress on switches, leading to greater efficiency and reduced size. Nevertheless, its performance limited by specific coupled-inductor design requirements, which also make difficulty for a specific power and voltage levels. **Yu-En Wu *et al* (2022)** [19] have presented a three-port BDC with a coupled inductor coordinates the DC bus step-down mode, PV and battery step-up mode for high conversion ratios, high efficacy with recycling of energy from leakage inductance, and reduced transformer voltage stress. However, the operation of this converter requires the precise coordination of control of the three ports to maintain stability under varying load and source conditions. **Jingang Han *et al* (2020)** [20] have implemented an H-bridge based BDC converter to enable battery charging and discharging, and operate efficiently at a broad range of voltages. The design included a PI control strategy for stable operation, and included a duty ratio feed forward control method to improve charging, discharging, and reversing power flow.

However, if the feed forward parameters are not tuned correctly, and slower transient response and less accurate control result.

As a result, in this research, a MB-SLC with cascaded PI controllers has been proposed, which addresses the limitations of existing approaches, to deliver the higher voltage gain, a decrease in ripple, and a more efficient and controlled bidirectional management of energy flow between DC supply and battery pack. The contribution of this work are,

- DC supply derived from renewable resources such as PV and wind, act as the primary clean energy source.
- MB-SLC performs a buck and boost operation, enabling bidirectional power transfer between the DC source and battery pack while maintaining a stable output voltage and maintaining high efficiency.
- Boost control loop is created with a cascaded PI controller to control the DC bus voltage via an outer loop and control the inductor current accurately using the inner loop to control the step-up operation accurately.

- Buck control loop is implemented as a cascaded PI controller, generates reference current with outer voltage loop and controls the inductor current with an inner loop to allow for accurate step-down power transfer.
- SOC-based PI controller continuously tracks the battery's SOC and regulates both charging and discharging, increase the battery life and preventing conditions of overcharging and deep discharging.
- PWM generator, which produces switching pulses from the PI controller signals, allows for accurate modulation.
- Battery pack stores surplus energy during excess generation and supplies it back during lower generation, thus maintaining system reliability, balancing supply demand fluctuations, and prolonging the energy availability.

## II. PROPOSED SYSTEM DESCRIPTION

The proposed system initiates with the input DC supply, which is the main energy source for the overall system as displays in Fig. 1. The DC voltage supply stated from renewable sources including PV panels, wind or any other DC generating system. The supplied voltage is applied to a Multiport Bidirectional SEPIC-Luo Converter which performs either a step-up (boost) or step-down (buck) operation depending on power flow requirements. The converter also manages bidirectional energy transfer between the input source and Battery Pack for charging and discharging. The Battery Pack, which stores surplus power from generation when it exceeds the demand and then discharge during insufficient generation. The converter continuously monitor DC bus voltage and battery SOC to maintain optimal operation.

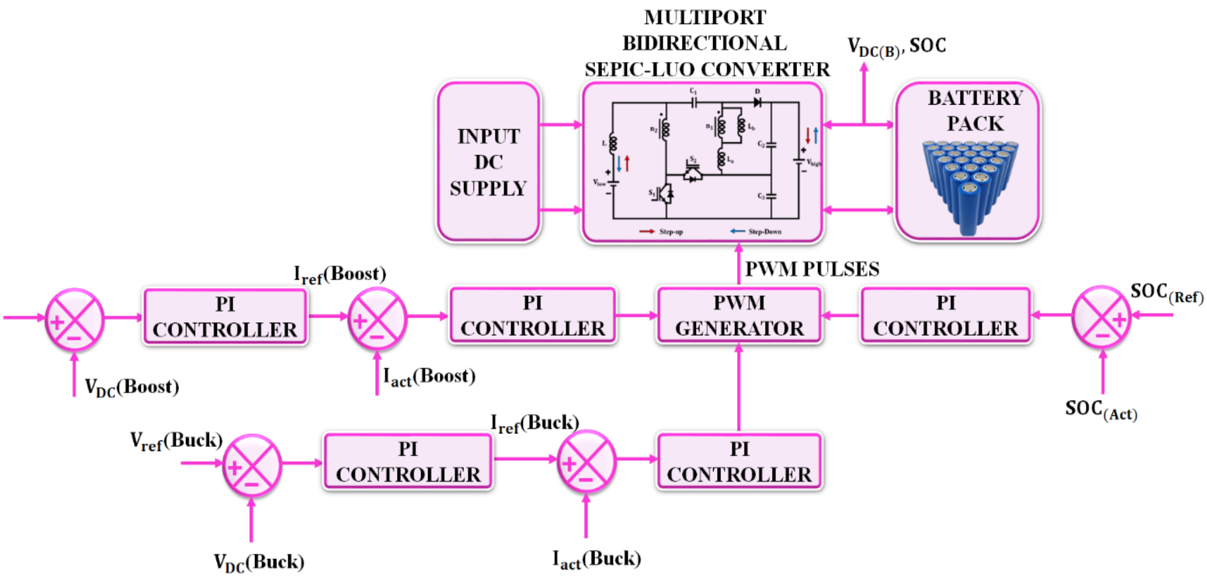


**Fig. 1. Proposed block diagram of energy management system using MB-SLC.**

The control system managed by PI Controllers to accurately control voltage, current, and SOC.

In this system has separate control loops are implemented for boost and buck operation.

For boost operation, a cascaded PI controller consists of an outer voltage loop that compares the boost reference voltage with actual DC bus voltage, thus generates a reference current, and similarly an inner loop that compares the reference current with actual inductor current to control the step-up operation.

For buck operation, a cascaded PI controller compares buck reference voltage with actual buck-side voltage and produces a reference current, which is regulated inner loop to allow for the step-down operation. For SOC management, a separate PI controller compares SOC reference with actual SOC to decide charging and discharging operation. The control outputs are directed to PWM generator, which is deliver switching pulses for the converter, ensuring efficient energy management, stabilize voltage, and battery protection.

## III. PROPOSED METHODOLOGY

### *A. Multiport Bidirectional Sepic–Luo Converter (MB-SLC)*

The converter topology shown in Fig. 2 is efficient and contains a bidirectional switches $(S_1 \text{ and } S_2)$, capacitors $(C_1, C_2 \text{ and } C_2)$, inductor $L, L_a \text{ and } L_b$.

The converter interconnects two voltage ports, $V_{Low}$ representing the lower voltage and $V_{High}$ representing the higher voltage. The converter operates in both the step-down (Luo) and step-up (SEPIC) bidirectional, with power flowing from either port.

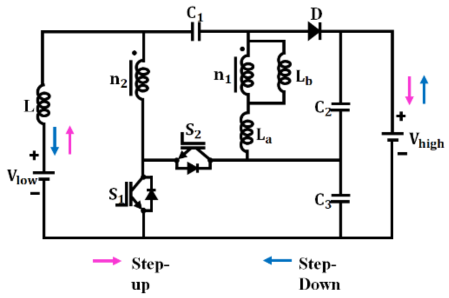


**Fig. 2. Circuit diagram of multiport bidirectional SEPIC-Luo converter.**

**Step-up conversion Process:**

These operational features have two switching states, thus the power is moved from $V_{Low}$ to $V_{High}$, as described in detail below:

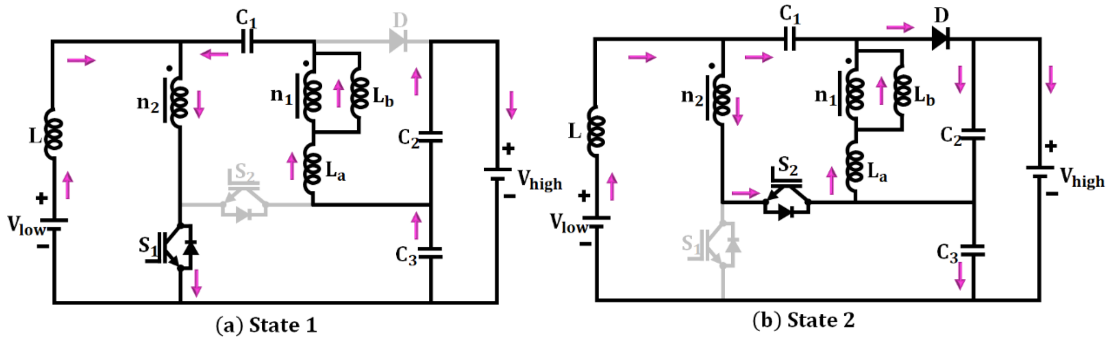


**Fig. 3. Equivalent Circuit of Step-up mode (a) state 1 (b) state 2.**

**State 1**: $S_1$ switched ON and $S_2$ turned OFF. As a result, $L$ experiences a positive voltage and increased current. Subsequently, voltage over the primary side of a linked inductor equals to voltage difference between $C_1, and\ C_3$, which is negative. The load $R_o$ is powered by $C_2$ current. Fig. 3(a) shows the present route of this switching condition.

$$V_L = V_{Low} - NV_{Lm} \tag{1}$$

$$V_{Lb}(1-N) = V_{C1} - V_{C3} \tag{2}$$

$$V_{High} = V_{C2} + V_{C3} \tag{3}$$

$$i_{Low} = i_{S1} + i_{C1} \tag{4}$$

$$i_{C2} = -i_{High} \tag{5}$$

$$i_{C3} = i_{La} - i_{High} \tag{6}$$

**State 2:** The switching condition when $S_1$ is switched OFF and $S_2$ is switched ON. The voltage through $L$ generated by negative, resulting in decreased current. The voltage through primary side of a linked inductor is positive, resulting in increased $L_a\ and\ L_b$ currents. The linked inductor's secondary winding stores energy, which charges $C_1$. Additionally, energy kept in $L_a\ and\ L_b$ is transmitted to $C_2, C_3\ and\ R_O$. Fig. 3(b) depicts the corresponding circuit in this state, which yields the formulas below:

$$V_{Lb} = V_{C2} \tag{7}$$

$$V_L = V_{Low} - V_{C3} - NV_{C2} \tag{8}$$

$$V_{C1} = V_{Lb}(1-N) \tag{9}$$

$$i_D = i_{High} + i_{C2} \tag{10}$$

$$I_{C3} = i_{Low} - i_{High} \tag{11}$$

$$i_{C1} = -(i_D + i_{La}) \tag{12}$$

$$i_{n2} = i_{S2} \tag{13}$$

**Step-down conversion Process:**

The step-down operation has two switching states, both states transfer power from $V_{High}$ to $V_{Low}$ The output load is $R_O$.

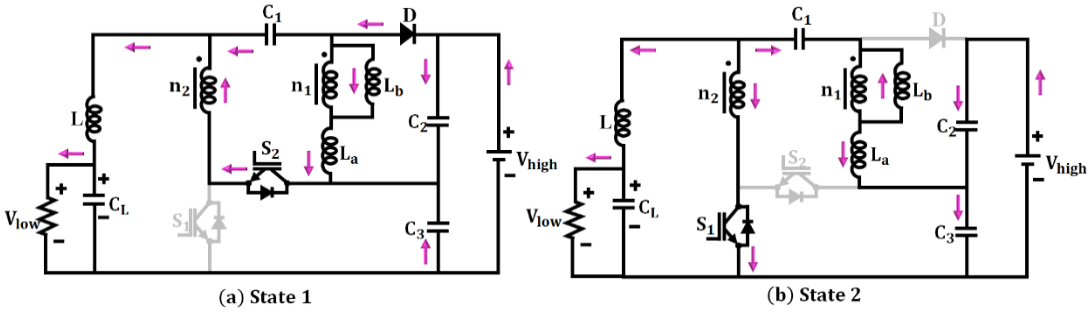


**Fig. 4. Equivalent Circuit of Step down mode (a) state 1 (b) state 2.**

**State 1:** Switch $S_2$ is ON and $S_1$ is OFF. Under this condition, diode $D$ is forward-biased and conducts. Current in inductor $L$ is increasing as energy from $V_{High}$ flows to capacitor $C_2$, the coupled inductor, and the load $R_o$ through $S_2$ and $D$. Capacitors $C_1$ and $C_3$ are discharging at this point. Fig. 4(a) depicts the current motion of this state, from which subsequently derive the equations.

$$V_L = V_{C3} + NV_{C2} - V_{Low} \tag{14}$$

$$i_{High} = i_D + i_{C2} = i_{La} + i_{C1} + i_{C2} \tag{15}$$

$$i_L = i_{S2} + i_{c1} = i_{low} + i_{CL} \tag{16}$$

**State 2:** This switching state when switch $S_2$ is OFF, switch $S_1$ is ON, and diode $D$ becomes reverse-biased. In this phase of the step-up mode, the voltage across inductor $L$ turns negative and offers a negative voltage to current flowing through it. With a positive voltage through primary side of $L_a$ *and* $L_b$ inductor currents, both increase. During this process, capacitors $C_1$ and $C_3$ are charged with energy being released from the inductor. Fig. 4(b) is illustrated in corresponding structure of state 2 in step-down mode.

$$V_L = NV_{Lb} - V_{Low} \tag{17}$$

**Static Performance analysis:**

Proposed converter is analyzed in term of its voltage gain for both step-up and step-down development with expression delivered for peak switching voltage stress on devices and current flow through the circuit components.

Under the assumption of applying volt–second balance law on the inductor $L_b$ expressed as:

$$V_{LbT_s} = 0 \rightarrow D_1\left(\frac{V_{C1} - V_{C3}}{1-N}\right) + (1-D_1)\frac{V_{C1}}{1-N} \tag{18}$$

Following the simplification of (18), the capacitor voltage $C_1$ is stated in $V_{C3}$:

$$V_{C1} = D_1 V_{C3} \tag{19}$$

Capacitor voltage $C_1$ is stated in $V_{C2}$:

$$V_{C1} = (1-N)V_{C2} \tag{20}$$

Applying volt-second law on $L$, the flowing relation is attained:

$$V_{LT_s} = 0 \rightarrow D_1 V_{Low} + D_1\left(\frac{N(1-D_1)}{1-N}V_{C3}\right) + (1-D_1)V_{Low} = 0 \tag{21}$$

Simplifying (22), the capacitor voltage $V_{C3}$ is given terms of $V_{Low}$ and the duty cycle:

$$V_{C3} = \frac{V_{Low}}{1-D_1} = \frac{V_{Low}}{D_2} \tag{22}$$

Therefore, voltage of $C_1$ and $C_2$ expressed as:

$$V_{C1} = \frac{D_1 V_{Low}}{1-D_1} \tag{23}$$

$$V_{C2} = \frac{D_1 V_{Low}}{(1-D_1)(1-N)} \tag{24}$$

Finally, high voltage port and step-up voltage gain are computed as follows:

$$V_{High} = V_{C2} + V_{C3} = \frac{D_1 + (1-N)}{D_2(1-N)}V_{Low} \tag{25}$$

$$M = \frac{V_{High}}{V_{Low}} = \frac{D_1 + (1-N)}{D_2(1-N)} \tag{26}$$

Similarly, following the technique, the capacitor voltage and step-down voltage gain are acquired:

$$V_{C1} = \frac{1-N}{(1-D_2)+(1-N)} V_{High} \quad (27)$$

$$V_{C2} = \frac{1-D_2}{(1-D_2)+(1-N)} V_{High} \quad (28)$$

$$V_{C3} = \frac{(1-N)(1-D_2)}{(1-D_2)+(1-N)} V_{High} \quad (29)$$

The step down voltage gain is given by:

$$M = \frac{V_{Low}}{V_{High}} = \frac{D_2(1-N)}{D_1+(1-N)} \quad (30)$$

The peak voltage across $S_2$ is derived from state 1 of the step-up mode:

$$V_{S2} = V_{C1} + (1-N)V_{Lb} = \frac{V_{Low}}{D_2} \quad (31)$$

The maximum voltage across switch $S_1$ is considered from state 2 of the step-up mode:

$$V_{S1} = V_{C3} = V_{S2} = \frac{1-N}{D_1+(1-N)} V_{High} \quad (32)$$

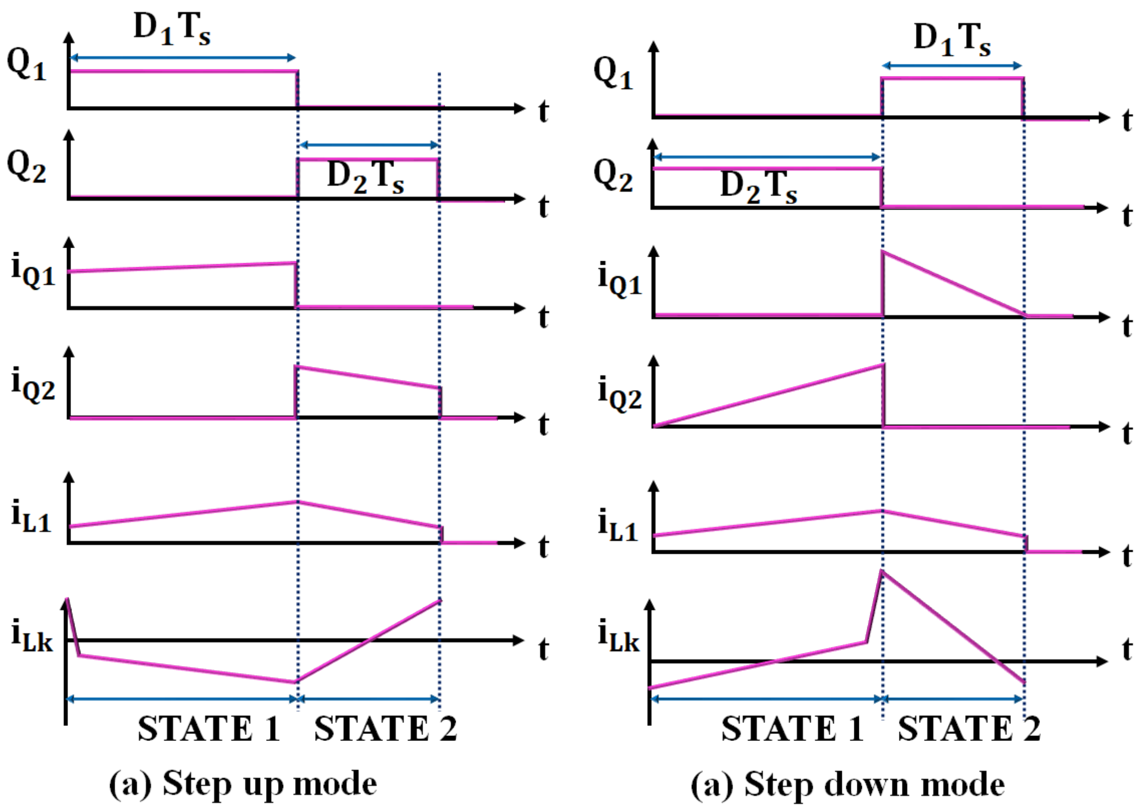


**Fig. 5. Switching waveforms (a) Step up mode (b) Step down mode.**

Fig. 5 (a) and (b) display main waveforms of proposed converter in the step-up and step-down operation modes, individually.

It is potential for high voltage gain with low component stress, making it highly effective for power conversion using renewable energies and in applications such as EVs.

In designing and regulating this converter to ensure stable output performance, a PI controller is utilized.

*B. PI Control Strategy*

**Cascaded PI control strategy for boost and buck regulation**

The proposed MB-SLC system incorporates a cascaded PI control scheme, outer voltage loop computes a reference current, while inner current loop controls the inductor current by modulating switching duty cycle, thereby ensuring accurate buck and boost operation and battery charging and discharging control. A cascaded PI control structure is used for both buck and boost mode, with outer voltage loop computing a reference current and inner current loop maintaining inductor current by adjusting duty ratio. Fig. 6 illustrates a control loop of cascaded PI controller.

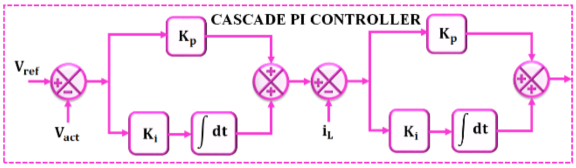

**Fig. 6. Basic structure of cascaded PI controller.**

The dual-loop structure improves system dynamics, as the fast inner current loop quickly suppresses disturbances before they affect the slower outer voltage loop. Assume that the inner loop bandwidth is approximately ten times larger than the outer loop bandwidth, thereby achieving fast current dynamics but still permitting stable voltage regulation and accurate battery state of charge management. The PI controllers for both of these loops written in the general form,

$$G_{PI}(s) = K_p + \frac{K_i}{s} = \frac{K_p s + K_i}{s} \quad (33)$$

Here $K_p$ and $K_i$ denotes proportional and integral gains, respectively. The outer voltage loop PI controller's transfer function written as follows:

$$G_{outer}(s) = \frac{K_{p,v} s + K_{i,v}}{s} \quad (34)$$

While the inner current loop PI controller is expressed as,

$$G_{inner}(s) = \frac{K_{p,v} s + K_{i,i}}{s} \quad (35)$$

In the boost mode, which manages the charging operation through SEPIC stage, the outer loop acts as a voltage controller, where reference DC bus voltage is compared with dignified bus voltage.

The error is managed via a PI controller for duty ratio of switching devices to adjust the charging current provided to battery pack. Effectively, in boost operation, battery is delivering power to DC bus when the input generation from source generation input is insufficient.

The outer PI controller compares the reference DC bus voltage $V_{ref}$ with measured voltage $V_{dc}$ to generate a reference current $I_{ref}$.

$$e_v(t) = V_{ref} - V_{dc}(t) \quad (36)$$

The dynamics of the outer PI controller written as:

$$I_{ref}(s) = G_{outer}(s).E_v(s) = \left(K_{p,v} + \frac{K_{i,v}}{s}\right) \cdot E_v(s) \quad (37)$$

The inner current PI controller is track the reference current. Error in inductor current is:

$$e_i(t) = I_{ref}(t) - i_L(t) \quad (38)$$

Control signal (duty cycle) is:

$$d(s) = G_{inner}(s).E_i(s) = \left(K_{p,i} + \frac{K_{i,i}}{s}\right) \cdot E_i(s) \quad (39)$$

Therefore in boost mode, the cascade structure ensures the DC bus voltage is controlled hence that the battery is deliver all of the required current.

In Buck mode simply manages the discharging process through the Luo converter and cascades in the same way. The outer voltage loop compares buck side voltage with its reference value to produce a current reference. The inner loop then adjusts the duty ratio of Luo converter switches to ensure that the battery discharge current precisely tracks the reference. In buck operation, extra energy from a DC bus is serve for charging the battery while the outer loop regulates around the charging voltage/current reference for the battery. The voltage error is:

$$e_v(t) = V_{bat,ref} - V_{bat}(t). \quad (40)$$

The outer PI controller produces the reference charging current:

$$I_{ref}(s) = G_{outer}(s).E_v(s) = \left(K_{p,v} + \frac{K_{i,v}}{s}\right) \cdot E_v(s) \quad (41)$$

This reference is applied to inner current loop, which regulates the charging current into the battery:

$$e_i(t) = I_{ref}(t) - i_{bat}(t), \quad (42)$$

$$d(s) = G_{inner}(s).E_i(s) = \left(K_{p,i} + \frac{K_{i,i}}{s}\right) \cdot E_i(s) \quad (43)$$

Consequently, it determined that the PI controller ensures the battery is charged smoothly at a specified charging current while maintaining stability of the converter.

**SOC regulation through PI controller**

The SOC of the battery expressed the ratio of available charge relative to its related to its rated capacity, mathematically expressed as,

$$SOC(t) = SOC(0) + \frac{1}{Q}\int I_{ESS}(t)dt \quad (44)$$

Here, $Q$ denotes battery capacity and $I_{ESS}$ represents charging or discharging current of ESS. During buck mode, the converter operates charge the battery by controlling the charging current while boost mod, the converter enables the battery to discharge. The PI controller continuously regulates SOC by comparing the reference value within the actual SOC and generates control signals that are fed to the PWM generator, thus ensure balance charging and discharging operations.

*C. Battery*

A rechargeable battery system is employed, where single cells are combined into modules, and the multiple modules connected to the batteries. BESS collects energy from renewable energy sources and stores it for later uses. Whenever supply interruptions occurs, demand spikes, or renewable generation drops, the stored energy is released by batteries to facilitate the energy distribution. A simplified electrically connected battery model has been constructed in defects as using resistances, voltages and capacitors as in Fig. 7.

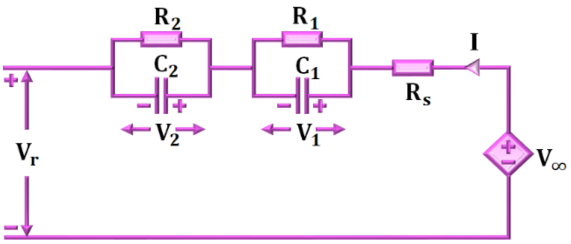


**Fig. 7. Equivalent circuit of battery.**

Using KCL in the circuit leads to equations (45) and (46).

$$V_1(t) = \frac{1}{R_1C_1}V_1(t) + \frac{I(t)}{C_1}. \quad (45)$$

$$V_2(t) = \frac{1}{R_2C_2}V_2(t) + \frac{I(t)}{C_2}. \quad (46)$$

The derivatives of voltage $V_1$ and $V_2$ are modified in $V_1(t)$ and $V_2(t)$. Using KVL in the circuit leads to Equation (47).

$$V_T(t) = V_{oc}(Z(t)) - V_1(t) - V_2(t) - R_sI_t \quad (47)$$

Here $V_{oc}$ stands open circuit voltage: $V_1$ and $V_2$ are the voltage drops parallel; and $R_s$ stands internal resistance. The proposed system shows great efficiency, dynamic response speed, ripple yield, and less components to maintain reliable bi-directional energy transfer to provide the large advantages relating to renewable energy and BESS.

## IV. RESULT AND DISCUSSION

The proposed MB-SLC has been validated for energy management bidirectionally with efficiency, stable voltage, current regulation, and SOC control. Its performance is evaluated in MATLAB/Simulink, which confirms that it is superior to conventional converters based on overall efficiency, the number of components reduced, and dynamic response time. Parameter specification of proposed work illustrates in Table1.

*Table* 1 Parameter Specifications

| Parameter | Specifications |
|---|---|
| **DC Source** | |
| DC Source Voltage | $12V$ |
| **MB-SLC** | |
| Switching Frequency | $10kHz$ |
| $C_1, C_2, C_3,$ | $22\mu F$ |
| $L, L_a, L_b$ | $4.7mH$ |

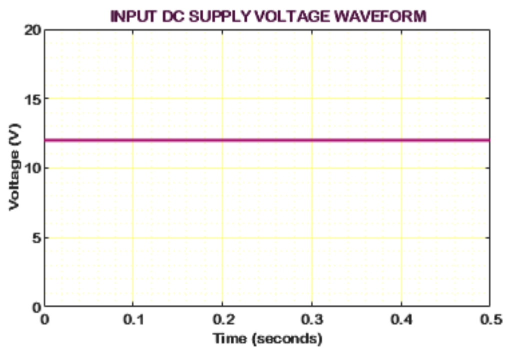


**Fig. 8. Input DC supply voltage waveforms.**

Fig. 8 illustrates input DC supply voltage waveform of the proposed system. The input supply voltage is maintained at approximately $12V$ for an entire simulation period of 0 to 0.5 seconds, demonstrating a steady and ripple-free input supply. It is an essential requirement for the MB-SL to have consistent DC input for dependable performance whilst in both buck and boost modes.

**Battery Side Boost Mode 1:**

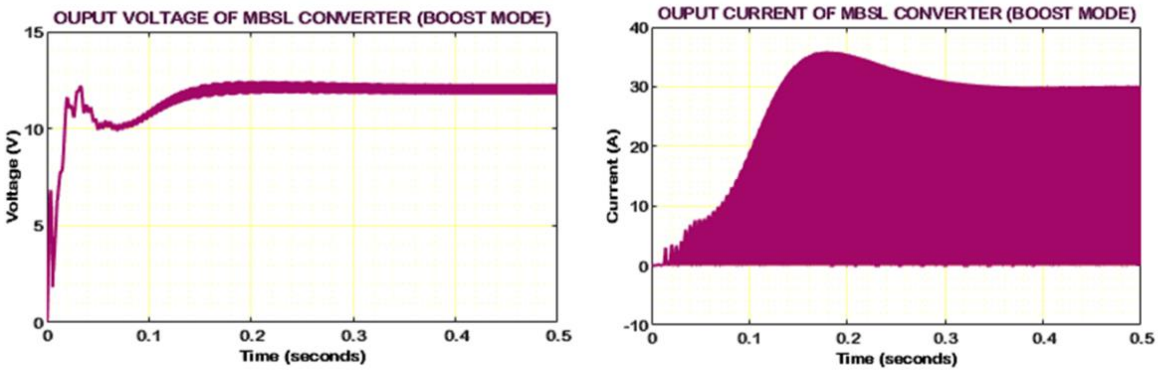


**Fig. 9. Output response for MB-SLC in boost mode.**

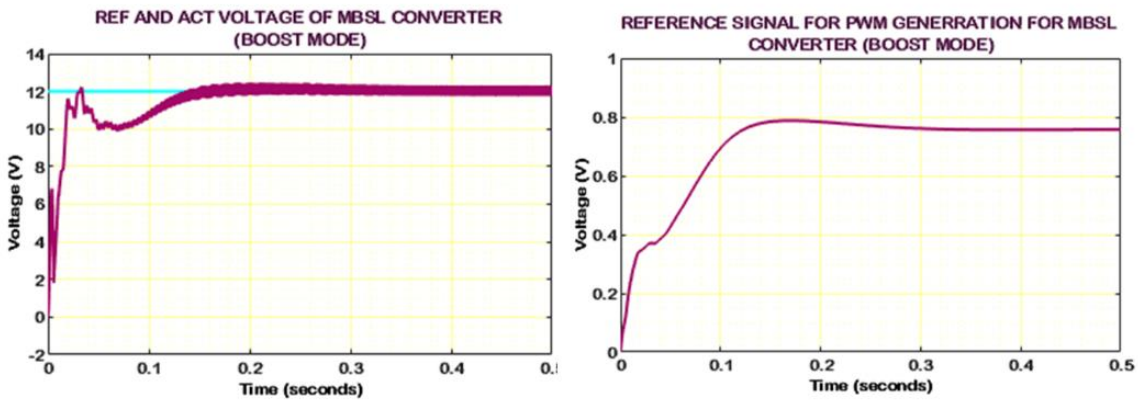


**Fig. 10. Reference tracking and PWM signal of MB-SLC in boost mode.**

Fig. 10 displays reference tracking and PWM signal of the MB-SLC during boost mode. The reference and actual output voltage, where the output of converter quickly rises and settles at $12V$ and thoroughly monitors the reference with little steady-state error, providing evidence for the PI control implementation. The PWM reference signal that stabilizes after the transient at $0.78V$, showing that switching is triggered properly and is stable during the boost operation.

**Battery Side Buck Mode 2:**

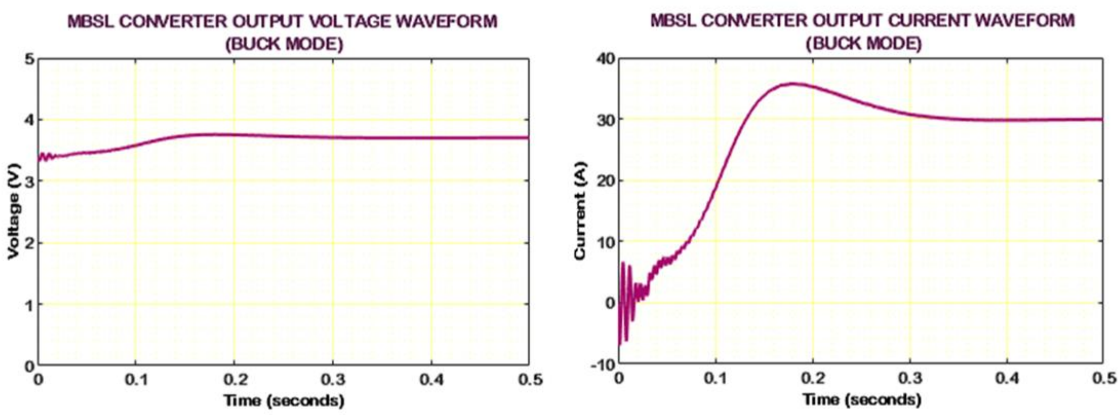


**Fig. 11. Output response for MB-SLC in buck mode.**

The MB-SLC's buck mode behaviors are shown in Fig. 11. The output voltage settles at $3.8V$ with minimal oscillation, which indicates stable step-down regulation. The output current rises quickly at $35A$ at time 0.15 s and then settles to $30A$. This shows that the MB-SLC mode is effective in buck operation for dynamic response and current regulation.

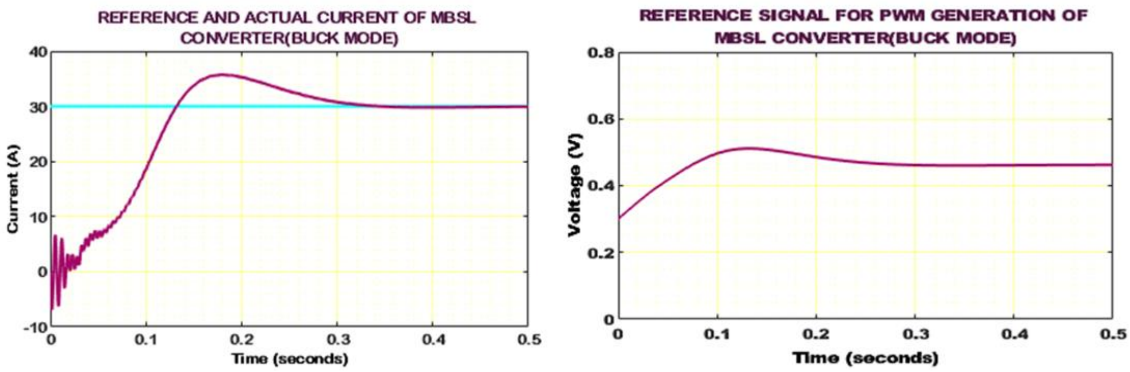


**Fig. 12. Reference tracking and PWM signal of MB-SLC in buck mode.**

Fig. 12 represents reference tracking and PWM signal of the MB-SLC in buck mode. The actual current tracks the reference current closely and smoothly settles to nearly $30A$ with small steady-state error indicative of the PI control being accurate. The PWM reference signal stabilizes at $0.45V$ after the initial transient, confirming that the duty cycle modulation is accurate and stable operation in the buck mode.

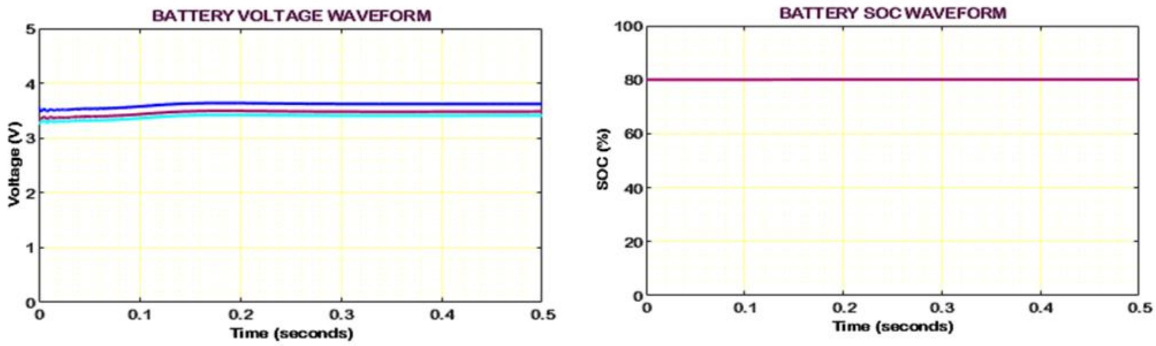


**Fig. 13. Battery performance.**

Fig. 13 represents the battery performance of the MB-SLC.

The battery voltage waveform, which stabilizes around $3.8V$ with minimal ripple, that properly regulated a charging and discharging operations.

The battery SOC remains consistent at 80 % throughout the simulation time, confirming that the PI based control strategy is effective at maintaining the desired SOC level and avoiding an overcharge and deep discharge condition.

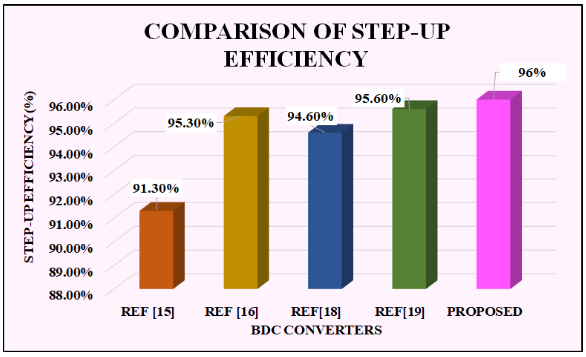


**Fig. 14. Comparison of Step up efficiency.**

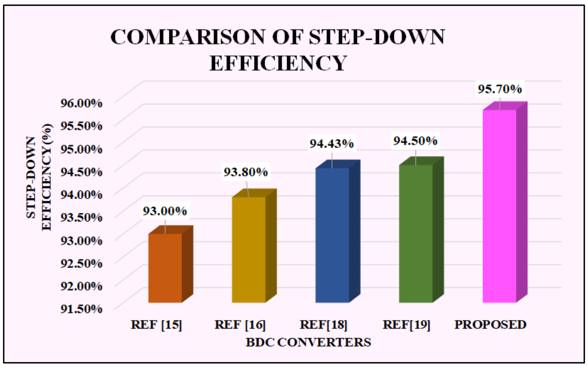


**Fig. 15. Comparison of Step down efficiency.**

Fig. 14 and 15 represents the efficiency comparisons of the MB-SLC and existing converters. For the step-up efficiency, the proposed converter attained a maximum value of 96 %, which is greater than Ref. [15] (93 %), Ref. [16] (93.8 %), Ref. [18] (94.43 %), and Ref. [19] (94.5 %). For the step-down efficiency, the proposed system achieved better performance at 95.7 % compared than Ref. [15] (93.0 %), Ref. [16] (93.8 %), Ref. [18] (94.43 %), and Ref. [19] (94.5 %). These results demonstrate that the MB-SL converter achieves improved efficiency for both boost and buck modes, which substantiates the MB-SL converters performance versus conventional designs.

*Table* 2 Converter components comparison

| Converters | Switch | Diode | Inductor | Capacitor | Total components |
|---|---|---|---|---|---|
| REF [21] | 4 | 5 | 5 | 4 | 18 |
| REF [17] | 4 | - | 8 | 2 | 14 |
| REF [22] | 4 | 2 | 4 | 3 | 13 |
| REF [23] | 4 | - | 5 | 3 | 12 |
| PROPOSED | 2 | 1 | 5 | 3 | 11 |

Table 2 illustrates component comparison of proposed converter against existing topologies. The proposed MB-SLC uses only 11 components (2 switches, 1 diode, 5 inductors, and 3 capacitors), which is fewer than Ref. [21] (18 components), Ref. [17] (14 components), Ref. [22] (13 components), and Ref. [23] (12 components). The significant reduction in total components illustrates the simplicity and cost-effective nature of the proposed design, ensuring added reliability, small size, and ease of implementation, when compared to standard converters.

## V. CONCLUSION

The proposed MB-SLC with cascaded PI control has been successfully designed and analyzed for effective energy management of renewable-based systems. With the aid of MB-SLC, this system achieves stable bidirectional operation with superior voltage, high step up and step down efficiency, and decreases ripples. The performance of the PI controller, which delivers accurate voltage and current regulation that smoothly manages SOC level of a storage system, while providing stable bi-directional operation of coupled components under varying conditions. The results from MATLAB/Simulink validated its enhanced efficiency of 96% in boost mode and 95.7% in buck mode, along with a reduced ripple and lower number of components compared to other existing designs. These features enhance its reliability, compactness and low-cost substitute, add to the functional delivery of the proposed MB-SLC for extended application specifically, electric vehicles, BESS, and incorporation of clean energy sources.

## REFERENCES


[1] Zeng J., Du X., Yang Z. A multiport bidirectional DC–DC converter for hybrid renewable energy system integration. *IEEE Transactions on Power Electronics*, 2021, vol. 36, no. 11, pp. 12281-12291. https://doi.org/10.1109/TPEL.2021.3082427 .

[2] Li X., Wang S. Energy management and operational control methods for grid battery energy storage systems. *CSEE Journal of Power and Energy Systems*, 2019, vol. 7, no. 5, pp. 1026-1040. https://doi.org/10.17775/CSEEJPES.2019.00160 .

[3] Marei M. I., Alajmi B. N., Abdelsalam I., Ahmed N. A. An integrated topology of three-port DC-DC converter for PV-battery power systems. *IEEE Open Journal of the Industrial Electronics Society*, 2022, vol. 3, pp. 409-419. https://doi.org/10.1109/OJIES.2022.3182977 .

[4] Ancy K., Sarojini V., Christy A. J., Bakri M., El Manna C., Florence S. S., Vijilvani C., Bindhu M. R., Bai S. J. S. Antibacterial activities and photocatalyzed degradation of textile dyeing waste water by Mn and F co-doped TiO2 nanoparticles. *Advances in Natural Sciences:*

*Nanoscience and Nanotechnology*, 2022, vol. 13, no. 4, pp. 045005. https://doi.org/10.1088/2043-6262/ac9c53 .

[5] Ramesh P., Gouda P. K., Rameshbabu A., Ramanathan G., Bharatiraja C. An isolated multi-port bidirectional DC-DC converter for EV applications. *Materials Today: Proceedings*, 2022, vol. 68, pp. 1853-1859. https://doi.org/10.1016/j.matpr.2022.08.047 .

[6] Marithangam A., Sarojini V. P., Al Farraj D. A., Elshikh M. S., Arokiyaraj S. Essential Oils from Citrus Fruit Peels to Control Foodborne Bacteria in Fresh-cut Guava Fruits. *BioResources*, 2025, vol. 20, no. 2, pp. 2587. https://doi.org/10.15376/biores.20.2.2587-2608 .

[7] Lee Y. R., Kang H. J., Kim M. K. Optimal operation approach with combined BESS sizing and PV generation in microgrid. *IEEE Access*, 2022, vol. 10, pp. 7453-27466. https://doi.org/10.1109/ACCESS.2022.3157294 .

[8] Kar S., Lins A. W., Patwa S., Martin G. W., Karthikeyan D. Modified Zeta Based PV System For EV Battery Charging. *In 2023 International Conference on Energy, Materials and Communication Engineering (ICEMCE)*, 2023, pp. 1-6. https://doi.org/10.1109/ICEMCE57940.2023.10434022 .

[9] Priya A. K., Yazhini A. Integrating Whale Optimization Algorithm and Machine Learning for Efficient Traffic Management. *International Journal of Advanced Trends in Engineering and Management (IJATEM)*, 2023, vol. 02, no. 10, pp. 12-23. https://doi.org/10.59544/ldhu1294/ijatemv02i10p2

[10] Pourjafar S., Shayeghi H., Sedaghati F., Seyedshenava S., Blaabjerg F. A bidirectional multiport DC-DC converter applied for energy storage system with hybrid energy sources. *International Journal of Circuit Theory and Applications*, 2021, vol. 49, no. 8, pp. 2453-2478. https://doi.org/10.1002/cta.2988 .

[11] Prabhu M. A., Sheela G. E., Alzahrani H., Siddiq H., Okmi A., Alharbi N., Florence S. S., Lekshmy M. S., Velayuthan Pillai S. Green synthesis of ZnO, Fe3O4, and TiO2 nanoparticles: exploring enhanced bacterial inhibition, catalysis, and photocatalysis for sustainable environmental applications. *International Journal of Environmental Analytical Chemistry*, 2024, pp. 1-25. https://doi.org/10.1080/03067319.2024.2404533 .

[12] Sreejyothi K. R., Chenchireddy K., Sydu S. A., Kumar V., Sultana W. Bidirectional battery charger circuit using buck/boost converter. *In 2022 6th International Conference on Electronics, Communication and Aerospace Technology*, 2022, pp. 63-68. https://doi.org/10.1109/ICECA55336.2022.10009062 .

[13] Kavin K. S., Karuvelam P. S., Kumar R. T., Sivasubramanian M., Kavitha P., Priyadharsini S. GWO Optimized PI Controller Fed PV Based Interleaved Luo Converter for EV Applications. *In 2023 14th International Conference on Computing Communication and Networking Technologies (ICCCNT)*, 2023, pp. 1-6. https://doi.org/10.1109/ICCCNT56998.2023.10307340.

[14] Almutairi A., Sayed K., Albagami N., Abo-Khalil A. G., Saleeb H. Multi-port pwm dc-dc power converter for renewable energy applications. *Energies*, 2021, vol. 14, no. 12, pp. 3490. https://doi.org/10.3390/en14123490 .

[15] Suresh K., Parimalasundar E., Arunraja A., Ellappan V., Ware E. T. High-efficiency stepdown/step-up converter for series-connected energy storage system. *Scientific Reports*, 2025, vol. 15, no. 1, pp. 7726. https://doi.org/10.1038/s41598-025-92234-y .

[16] Liao H., Chen Y. T., Chen L., Chen J. F. - Development of a bidirectional DC–DC converter with rapid energy bidirectional transition technology. Energies, 2022, vol. 15, no. 13, pp. 4583. https://doi.org/10.3390/en15134583 .

[17] Mousavinezhad Fardahar S., Sabahi M. High step-down/high step-up interleaved bidirectional DC–DC converter with low voltage stress on switches. *IET Power Electronics*, 2020, vol. 13, no. 1, pp. 104-115. https://doi.org/10.1049/iet-pel.2018.6164 .

[18] Malik M. Z., Zhang S., Hong Y., Alwahkyan A. R. A. Y., Ali A., Farooq A. A Coupled Inductor-Based Bidirectional DC-DC Converter with Step-Up Step-Down Operation for Electric Vehicle Applications. *International Transactions on Electrical Energy Systems*, 2023, vol. 2023, no. 1, pp. 9277881. https://doi.org/10.1155/2023/9277881 .

[19] Wu Y. E. Novel high-step-up/step-down three-port bidirectional DC/DC converter for photovoltaic systems. *Energies*, 2022, vol. 15, no. 14, pp. 5257. https://doi.org/10.3390/en15145257.

[20] Han J., Gu X., Yang Y., Tang T. Dynamic improvement with a feedforward control strategy of bidirectional DC-DC converter for battery charging and discharging. *Electronics*, 2020, vol. 9, no. 10, pp. 1738. https://doi.org/10.3390/electronics9101738 .

[21] Wu Y. E., Hsiao S. L. Novel high-efficiency three-port bidirectional step-up/step-down DC–DC converter for photovoltaic systems. *Sustainability*, 2021, vol. 13, no. 14, pp. 7913. https://doi.org/10.3390/su13147913

[22] Kadhim Almohammed A. Q., Delshad M., Bachache N. K., Fani B., Saghafi H. A new

SEPIC-Zeta bidirectional converter with high efficiency for renewable energy systems. *Hydrogen, Fuel Cell & Energy Storage*, 2024, vol. 11, no. 3, pp. 142-152. https://doi.org/10.22104/hfe.2024.6809.1292 .

[23] Abolhassani P., Maalandish M., Nadermohammadi A., Sharifian M. B. B., Feyzi M. R., Hosseini S. H. A high step-up high step-down coupled inductor based bidirectional DC–DC converter with low voltage stress on switches. *IET Power Electronics*, 2024, vol. 17, no.7, pp.802-823.
https://doi.org/10.1049/pel2.12694

## Information about authors

**R. V. L. N. S. Parvathi** working as an Assistant Professor at Godavari Institute of Engineering & Technology (Autonomous), Rajahmundry. Her main area of interest includes, Power Electronics and renewable energy systems.
Email: rvlnsparvathi@gmail.com
ORCID ID: 0009-0003-8023-7795

**Kunche Gowthami** is working as an Assistant Professor. Her main area of interest includes Power Electronics and Electrical Machines.
Email:gowthami75.k@gmail.com
ORCID ID:0000-0002-1166-5687

**Patta Tejeswararao** - UG student. His main area of interest includes, Power Electronics and renewable energy systems.
Email:pattatejeswararao721@gmail.com
ORCID ID: 0009-0006-2781-4604

**Gorrela Abhishek** UG student. His main area of interest includes, Power Electronics and renewable energy systems.
Email: shek45103@gmail.com

ORCID ID: 0009-0000-5839-0476

**Eluri Siva Naga Subramanyam** UG student. His main area of interest includes, Power Electronics and renewable energy systems.
Email:yelurisubbu143@gmail.com
ORCID ID: 0009-0007-0826 0703